# Realization and Properties of Biochemical-Computing Biocatalytic XOR Gate Based on Enzyme Inhibition by a Substrate

Jan Halámek, Vera Bocharova, Mary A. Arugula, Guinevere Strack, Vladimir Privman, and Evgeny Katz*

Department of Chemistry and Biomolecular Science, and Department of Physics, Clarkson University, Potsdam, New York 13699, United States

ABSTRACT: We consider a realization of the **XOR** logic gate in a process biocatalyzed by an enzyme which can be inhibited by a substrate when the latter is inputted at large enough concentrations. A model is developed for describing such systems in an approach suitable for evaluation of the analog noise amplification properties of the gate. The obtained data are fitted for gate quality evaluation within the developed model, and we discuss aspects of devising **XOR** gates for functioning in "biocomputing" systems utilizing biomolecules for information processing.
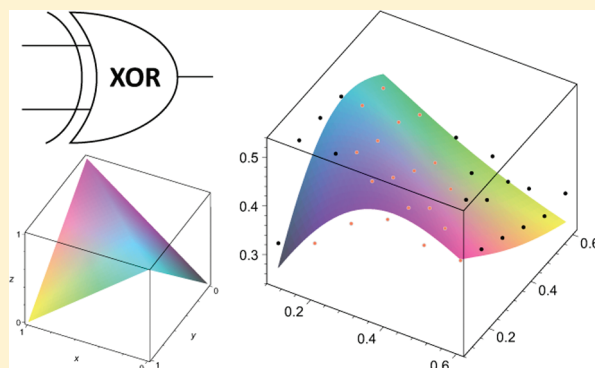
1. INTRODUCTION

Chemical computing,[1−7] i.e., processing of information with chemical reactions, has been an active area of unconventional computing.[8,9] Several chemical systems carrying out Boolean logic gates, such as **AND**,[10,11] **OR**,[12] **NAND**,[13,14] **NOR**,[15−18] **INHIB**,[19−22] **XOR**,[23−26] have been demonstrated. Biochemical computing[27−29] has utilized biomolecular kinetics for information processing, realizing binary logic gate functions and few-gate networks based, for instance, on proteins/enzymes,[30−38] antigens/antibodies,[39,40] DNAzymes,[41,42] DNA,[43,44] RNA,[45−49] and whole cells.[50] Biocomputing systems offer approaches to design multisignal responsive biosensors[51−53] and bioactuators[54,55] processing complex patterns of biochemical signals, for potential biomedical applications.[56−59]

XOR (eXclusive **OR**) gate has been a binary logic operation most difficult for (bio)chemical realizations.[60] Indeed, **XOR** is expected to yield output **0** when the two inputs are applied at zero levels (input combination **0,0**). When only a single input signal is applied at level **1**, output **1** is expected (system "activation" for input combinations **0,1** and **1,0**). However, simultaneously applying both inputs at level **1**, keeps the system inactive: output **0** (for inputs **1,1**). Therefore, unlike other recently realized[10−22] chemical gates (**AND**, **OR**, **NAND**, **NOR**, and **INHIB**), the **XOR** function involves an inherently nonmonotonic chemical output in response to increasing concentrations of the two chemical inputs.[60] In (bio)chemical setting this requires reactions with kinetics such that the effects of two input species cancel each other when they are both present in the system.

The **XOR** function has been realized by mutual negation of the chemical inputs which drive molecular restructuring, such as acid and base.[23,24] In supra-molecular systems input signals resulted in a change of a chemical complex's structure, measured by changes in optical absorbance or fluorescence, as each input binds at different sites of the complex, whereas binding of both of them resulted in no changes in the optical properties.[25,26] Biomolecular realization can be based on biorecognition or biocatalytic properties of DNA[48] or enzymes.[60−64] In "signal change" enzyme-based **XOR** gates[38,60−63] oppositely directed biocatalytic reactions are driven by input signals. Separate application of each chemical input unbalances the system, resulting in the output signal as a change in a measurable property. Both inputs, however, when present, drive competing reactions thus keeping the balance (no signal change). The resulting optical[60−63] or electrochemical outputs[38] require certain postprocessing in order to get the absolute value of the change as the **XOR** value. Such gates have been used as model systems[60] for **XOR** realizations. Here we consider a different approach whereby the nonmonotonic response is achieved by a suppression mechanism of the oxidative function of the enzyme HRP (horseradish peroxidase) at increased concentrations of its primary substrate, H_2O_2. The experimental details are given in section 2.

Despite the difficulties[60] in realizing the **XOR** gate in terms of single- or few-step (bio)chemical processes, explorations of its properties are important for several reasons. This gate is among the basic computing elements of half-adder/half-subtractor[65−68] or full-adder/full-subtractor.[69,70] These arithmetic functions were realized using DNA-based[71] and enzyme-based[64] processes. **XOR** is also a part of reversible gates: **CNOT**, **CCNOT**, etc., that have been utilized in other unconventional computing realizations.[72−77]

Furthermore, a response-surface function of a system that yields **XOR** output at the logic-point inputs **00, 01, 10, 11**, has a convoluted, saddle shape[60] as compared to other gates, such as **AND**. This matter is addressed in section 3, which also introduces a model that allows analysis of the noise-handling properties of our specific **XOR** realization. Generally, we expect[60] and confirm that the **XOR** gate is more noisy than **AND, OR** and other gates with less "structured" response surfaces. While the study of the noise handling by **XOR** gates is interesting, such gates will be candidates for inclusion in larger networks only provided noise suppressing elements (filters) are utilized, rather than being directly optimizable. Section 4 presents model fit and analysis of our data, discussion of the results, and offers concluding remarks.

2. EXPERIMENTAL: XOR GATE BASED ON ENZYME SUPPRESSION BY SUBSTRATE

Chemicals and Materials. Glucose oxidase (GOx) from *Aspergillus niger* type X-S (EC 1.1.3.4), horseradish peroxidase (HRP) type VI (EC 1.11.1.7), potassium hexacyanoferrate (II) trihydrate and D-(+)-glucose (99.5%) were purchased from Sigma-Aldrich and used without further purification. H_2O_2 (30% w/w) was purchased from Fisher. Ultrapure water (18.2 $M\Omega\cdot cm$) from NANOpure Diamond (Barnstead) source was used in all of the experiments.

Composition and Mapping of the XOR System. The main process of the **XOR** gate was based on 0.1 μM of enzyme HRP catalyzing the oxidation of 1 mM ferrocyanide by the "input" H_2O_2, in 10 mM phosphate buffer, pH 7.4. Glucose, preprocessed to yield the oxidizer, H_2O_2 (as described below and further explained in section 3), and additional directly introduced H_2O_2 were used as the two input signals. For both inputs, the logic value **0** was chosen as 0.1 mM and logic value **1**, as 0.6 mM.

For each experiment, input 1, glucose, was preprocessed in a separate cuvette by incubation with the 4.76 U mL^{-1} of GOx enzyme. The enzymatic reaction was continued for 15 min in the total volume of 2 mL with the constant air bubbling through the reaction solution. After that, 1 mL of the reaction mixture was transferred to another cuvette, where it was mixed with input 2. Input 2, H_2O_2, was directly added from the 100 mM stock by adjusting volume of transferred H_2O_2 solution according to the needs of experiment. Premixed solution of the inputs was transferred to an optical cuvette already containing HRP and ferrocyanide. The schematic illustration of the experimental setup is represented in Figure 1.

In the gate-response-mapping experiments the input signals were applied at (separately) variable concentrations, glucose, 0.1, 0.2, 0.3, 0.4, 0.5, and 0.6 mM and H_2O_2, 0.1, 0.2, 0.3, 0.4, 0.5, and 0.6 mM. There were thus 36 experimental data sets.

Optical Measurements. Absorbance, A, measurements were performed using a UV-2401PC/2501PC UV-Vis spectrophotometer (Shimadzu, Tokyo, Japan) at (25.0 ± 0.2) °C. The reaction was carried out in a 1 mL poly(methyl methacrylate), PMMA, cuvette for all of the different input combinations. The increase of absorbance was monitored as a function of time, at λ = 420 nm, resulting from the formation of ferricyanide due to oxidation biocatalyzed by HRP. A selection of our absorbance data is shown in Figure 2. The gate time, t_g = 60 s, was selected to obtain a well-defined **XOR** function, as further discussed in the following sections. In particular, for this time, input combinations
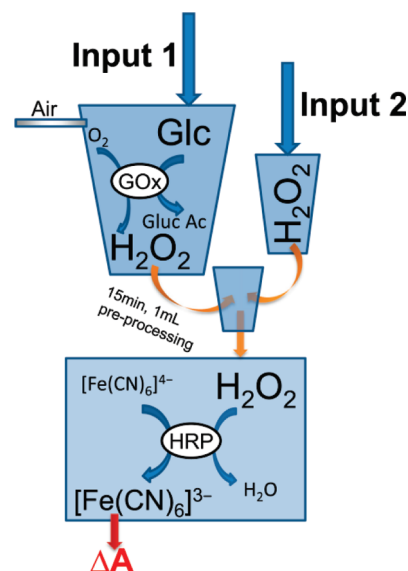

Figure 1. Biocatalytic cascade initiated by input 1, glucose (here marked as Glc), and input 2, H_2O_2, with the level of ferricyanide measured as the output signal of the **XOR** function. For this design input 1 was preprocessed with GOx in the cuvette of 2 mL with the air bubbled through the reaction solution. After 15 min of this enzymatic reaction in which H_2O_2 and gluconic acid (here marked as Gluc Ac) were produced, 1 mL of the resulting solution was transferred to another cuvette, where it was mixed with input 2. The premixed solution was then transferred to an optical cuvette in which ferrocyanide was oxidized by H_2O_2, by the biocatalytic action of HRP, to yield ferricyanide. The kinetics of formation of ferricyanide was optically monitored at λ = 420 nm.

0,0 and **1,1** give similar outputs which yields a good quality **XOR** function; see Figure 2.

Since some other chemicals can contribute to a limited extent, to the absorbance at λ = 420 nm, we used the change in the absorbance (ΔA) as compared to its value at time zero of the HRP step of the experiment, as the optical output measure. This in turn can be converted to the chemical output signal concentration, that of ferricyanide, denoted by $F(t)$, where t indicates its time-dependence, by using the Lambert-Beer law, where the molar extinction coefficient[78] of ferricyanide at λ = 420 nm is $\varepsilon_{420} = 1$ mM^{-1} cm^{-1}. The HRP concentration (0.1 μM) was also verified spectrophotometrically, where the molar extinction coefficient[79,80] of HRP at λ = 403 nm is $\varepsilon_{403} = 102$ mM^{-1} cm^{-1}. As explained in section 4, we used the experimental mean values of the logic-point **0** and **1** of the output at the gate time ($t_g = 60$ s), at the appropriate pairs of the "logic" inputs, to define $F_{min} = 0.32$ mM, $F_{max} = 0.41$ mM, used in shifting and scaling the output $F(t_g)$ to the logic range which ideally (if there were no noise in the data) should be between numerical 0 and 1, to draw the bar chart in Figure 2, which illustrates the degree of accuracy of the realized **XOR** function (see the next two sections for further discussion and references).

3. DESCRIPTION AND MODELING OF THE XOR GATE REALIZATION

As mentioned in section 1, among the binary logic gates realized in the framework of enzyme-catalyzed biochemical processes, **XOR** has been rather problematic, as detailed shortly. This puts in question the **XOR** gate's utility as a useful network
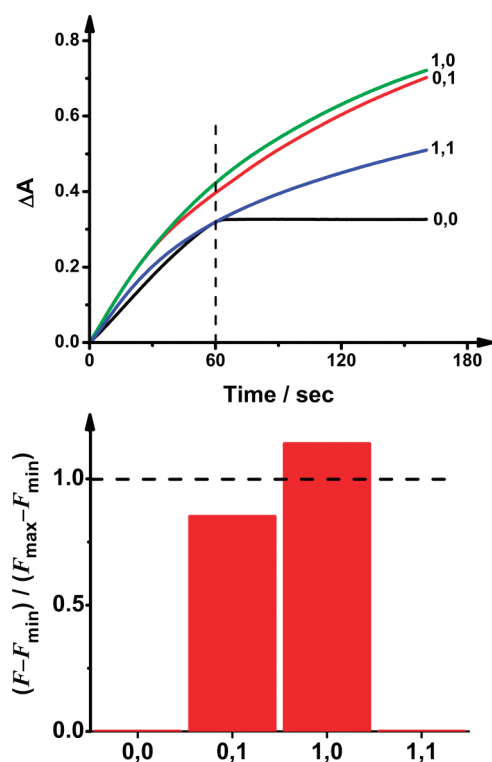
Figure 2. Time-dependent optical signals (top panel) measured as the change in the absorbance due to the production of ferricyanide, for the four "logic value" combinations of the two inputs: glucose and H_2O_2. For both inputs, logic **0** is taken at 0.1 mM and logic **1**, at 0.6 mM. Optical absorbance measurements were performed at λ = 420 nm. The bar chart (bottom panel) features the **XOR** logic realization at the selected gate time of 60 s. The vertical axis gives the ferricyanide concentration shifted and scaled in term of the logic-value range between values selected as **0** and **1** for the output, as explained in the text.

element for biochemical computing designs. However, experimental realizations of **XOR** gates and their analysis are of importance for general interest, as well as precisely for the purpose of cataloguing the challenges associated with design and adjustability of various component biochemical processes required to achieve complex information processing. The difficulty with the **XOR** gate (bio)chemical realizations has been traced to its truth table, shown below:

input1	input2	output	
0	0	0	
0	1	1	(1)
1	0	1	
1	1	0	

Indeed, most chemical and biochemical processes yield output which is a monotonically increasing function of the input chemical concentrations. Therefore, the fact that **XOR** requires output **0** at the $(1,1)$ inputs, necessitates the use of reactions with unusual properties or additional output-signal processing steps. Furthermore, such gates with two output values at **0** and diagonally positioned output values at **1**, have a more "structured" response surface, with therefore generally larger slopes (faster variation) than gates such as **AND**, the latter with the truth table containing only a single output **1**. As a result, the realized

XOR-type gates typically have stronger analog noise amplification[60] and are much more difficult to optimize for noiseless network functioning than **AND**-type gates.

In our earlier work,[60] an **XOR** gate was realized based on signal change, and its noise handling properties were investigated. That realization has required certain postprocessing, which was devised,[60] but not realized experimentally as a (bio)chemical step, in order to obtain the actual **XOR** response shown in truth table 1. Furthermore, its tuning for noise reduction also proved not straightforward. Indeed, after the signal postprocessing the "optimal" response surface of the signal-change gates approximates the one shown in Figure 3a, in terms of signal values in intervals scaled to the "logic" ranges between the binary 0 and 1, which are defined later in this section, which still has $\sqrt{2} \approx 140\%$ noise amplification factor per information processing step.[60] Here we explore another approach that yields response surfaces which are smooth functions that can approximate the ridged shape shown in Figure 3b, which has the same noise amplification factor (if accurately realized). In fact, it is unlikely that simple biochemical steps based on properties and functioning of one or few enzymes, can approximate the planar-face "origami" shape such as in Figure 3c, which would allow practically no noise amplification: all the faces shown have slopes 1. An even better shape is shown in Figure 3d: a sigmoidal "filter" version of the shape in Figure 3c, which has slopes less than 1 (means, analog noise suppression[81,82]) at all the logic points. This "saddle" shape for the **XOR** function would likely require a sequence of well-designed and tuned reaction processes of the complexity presently not realized in the (bio)chemical logic-gate literature.

In the present work, we realize the **XOR** function as shown in Figures 1 and 2. The enzyme, HRP, is known to be inhibited by too much of its substrate, H_2O_2. Therefore, we combine the two chemical signals, determined by the input chemicals of concentrations I_1 and I_2, into a single signal determined by $[H_2O_2]$, which in turn is driving the oxidation of a chromogen used to optically detect the output, the latter process catalyzed by HRP. As in the earlier, different realization,[60] the present **XOR** function is not carried out by a one-shot enzymatic process. Instead of the postprocessing, here we have preprocessing of the inputs. Actually, we preprocessed only one input, glucose, which was fed into a system producing H_2O_2, catalyzed by another enzyme, glucose oxidase (GOx); see Figure 1. The other input was taken directly as H_2O_2. Spatial separation and temporal "clocking" of biocomputing steps has received limited attention in the literature,[83] even though it has been realized[84] that these features are important for large-scale networking of biocomputing processes. However, it is also important to note that we are interested in information processing rather than the chemical kinetics aspects of these steps. Therefore, our preprocessing was carried out for long enough (fixed) time to ensure that all glucose is processed and equal quantity of H_2O_2 is produced. In terms of the concentrations of glucose and H_2O_2, the input I_1 is the same.

However, we note that such preprocessing and other "black box" (means, carried out identically without regard to the actual value of the input) information processing steps can be sources of *noise*, which is our primary topic of concern in this work. Therefore, while seemingly chemically trivial, such steps should be included if we want a realistic experiment as far as data noisiness is concerned. We chose one such input preprocessing step for the present work: Glucose $\rightarrow H_2O_2$; see Figure 1. The resulting data noisiness is illustrated in Figure 4. The actual kinetics is not interesting as far as information processing goes, and as mentioned,
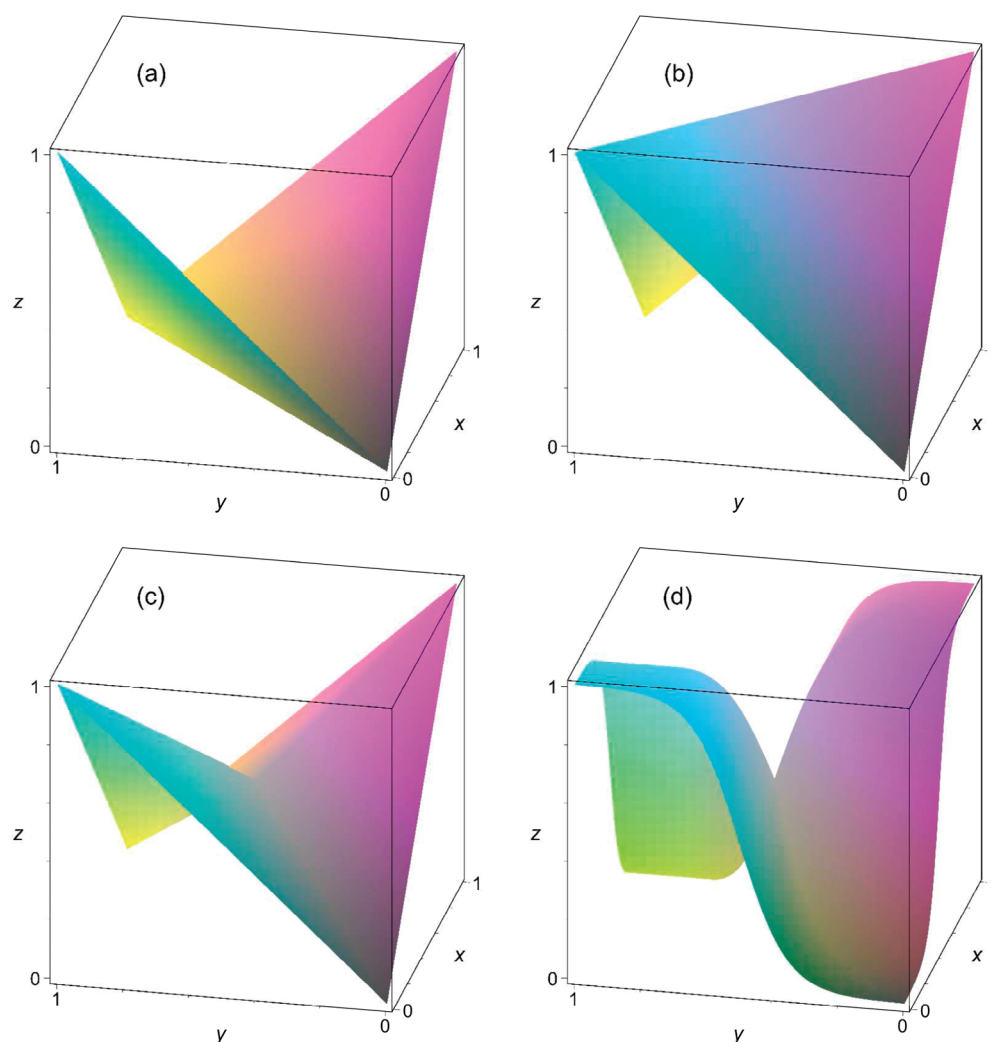
Figure 3. Response functions of interest in the **XOR** gate realizations. All the surfaces shown realize the **XOR** truth table, see eq 1. Experimentally realized: (a) the shown ridged shape can be approximately realized by the earlier-reported[60] signal-change **XOR** function, and has the optimal analog noise amplification factor, $\sqrt{2} > 1$, for such gates; (b) the shown ridged shape can be approximated by the **XOR** process realized in the present work. Not realized, and likely not realizable with single- or few-enzyme reactions: (c) an "origami" planar shape without noise amplification; (d) a "saddle" shape which would be optimal for noise-suppressing **XOR** gates.

we took the conditions such that the input, $I = [H_2O_2]$, into the second processing step, catalyzed by HRP, was $I = I_1 + I_2$.

We will use the following simple "cartoon" kinetic model to consider the parameter selections for the **XOR** function. As emphasized earlier,[27,60,81,82,85] analysis of the shape of response surfaces is frequently done with limited data and is aimed at an approximate global description of the function shape within a few-parameter model. Therefore, here we focus on two key features of the processes involved in the HRP functioning. We assume that the steps[86] of the enzymatic process which actually result in the oxidation of the chromogen, in our regime can be represented by a single-rate-constant irreversible production rate, $RE(t)$, which can be controlled by (is approximately proportional to) the instantaneous enzyme concentration. Approximately, we thus write the first term in

$$\frac{dI(t)}{dt} = -RE(t)I(t) - rI^2(t)E(t) = -[R + rI(t)]I(t)E(t)$$

(2)

We then assume (the second term) that the inhibition by H_2O_2, is approximately represented by that, some of the enzyme is "taken out of the game" by H_2O_2, at the rate $rI^2(t)$:

$$\frac{dE(t)}{dt} = -rI^2(t)E(t)$$

(3)

The latter process requires another molecule of H_2O_2. The quadratic in $[H_2O_2]$ rate expression is obviously an oversimplification of the actual inhibition process which involves[87,88] in part an intermediate complex of HRP (with H_2O_2) in the enzymatic cycle, being converted to an inert species as it further reacts with H_2O_2, and some other secondary and additional processes.[87,88] The proposed rate expression treats these processes in a cavalier way. The fact that ferrocyanide also competes for the same main complex is also not carefully considered. Technically, this should be reflected in that the rate r will depend on (decrease with) the initial ferrocyanide concentration.

We note that, while enzyme inhibition studies for "external" control of its function have a long history,[89−91] mechanistic

9841

dx.doi.org/10.1021/jp2041372 |*J. Phys. Chem. B* 2011, 115, 9838–9845

Figure 5. Plots of $F(t)$ as a function of I_0, for typical parameters reflecting our experimental conditions (see text), for several gate times $t = t_g = 20, 40, 60, 80,$ and 100 s, where increasing times give curves with larger values (of the output signal).
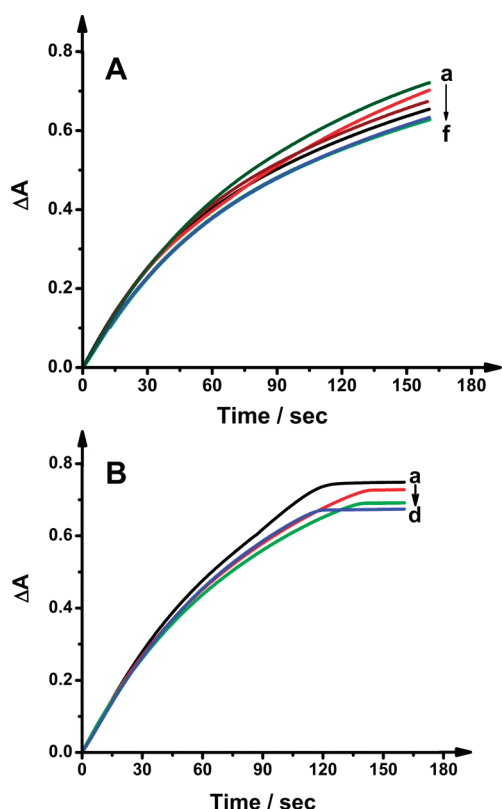
Figure 4. Data sets obtained for several combination so the inputs which, after the preprocessing of glucose should yield an identical overall H_2O_2 input into the second, HRP stage of the reaction (see Figure 1) and therefore, result in identical outputs. However, noisiness of the data results (in part) due to a different fraction of the overall H_2O_2 input fed directly vs that produced from the glucose-involving process by the action of GOx. Panel A presents kinetic (time-dependent) data for inputs: (a) glucose 0.6 mM and H_2O_2 0.1 mM; (b) glucose 0.1 mM and H_2O_2 0.6 mM; (c) glucose 0.5 mM and H_2O_2 0.2 mM; (d) glucose 0.2 mM and H_2O_2 0.5 mM; (e) glucose 0.4 mM and H_2O_2 0.3 mM; and (f) glucose 0.3 mM and H_2O_2 0.4 mM. Panel B presents data for: (a) glucose 0.1 mM and H_2O_2 0.4 mM; (b) glucose 0.4 mM and H_2O_2 0.1 mM; (c) glucose 0.2 mM and H_2O_2 0.3 mM; and (d) glucose 0.3 mM and H_2O_2 0.2 mM. Panel B illustrates that noise is present even in the saturation regime which is reached once the available H_2O_2 is used up, highlighting the property that the observed noise is at least in part due to different availability of H_2O_2 after the preprocessing in the GOx step.

results the specific inhibition mechanism considered here[87,88] have not been detailed enough to get information of the process parameters. Thus all of the rates have to be fitted from our data. The main virtue of the present "cartoon" model is that, it has few parameters (two rates). Another useful feature is that, at least in principle the model offers a prescription for how to change the rates: R, by varying the initial enzyme concentration to which this rate constant should be roughly proportional; r, by changing the initial ferrocyanide concentration, the increase of which will result in the effective value of r decreasing. We also note that the main effects of the inhibition occur during the initial time scales of the reaction when the concentration of H_2O_2 is not yet significantly depleted. Therefore, for purposes of the actual calculations we can further approximate the quadratic term by replacing
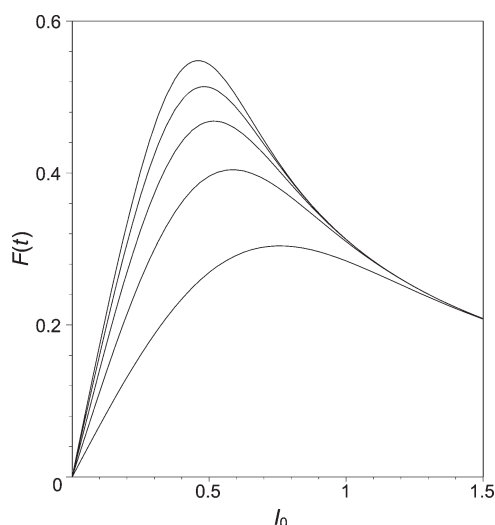
$$I^2(t) \rightarrow I(0)I(t) \qquad (4)$$

This makes the model analytically solvable, to yield, from

$$\frac{dF(t)}{dt} = 2RE(t)I(t) \qquad (5)$$

after a detailed calculation, the expression for the concentration, $F(t)$, of the produced ferricyanide,

$$F(t) = \frac{2I_0RE_0[1 - e^{rI_0^2t - (R + rI_0)E_0t}]}{(R + rI_0)E_0 - rI_0^2e^{rI_0^2t - (R + rI_0)E_0t}} \qquad (6)$$

where 5 is, within the present model, the rate of its production in the peroxidase cycle.[86] Here the time, t, is that of the HRP part of the experiment, and for brevity we denoted the initial concentrations $I_0 = I(0)$ and $E_0 = E(0)$.

The model eq 6, fits the time dependence of the measured data, $F(t)$, for each of the set of values of the initial inputs $I_{1,2}(0)$ with $E_0 = 10^{-4}$ mM and $I_0 = I_1(0) + I_2(0)$. However, we get large variations ($\pm 80\%$) in the effective values of the rates, which is an indication that the model is at best semiquantitative. Nevertheless, the model allows to illustrate the issues related to the selection of the **XOR** response shape from the nonmonotonic biochemical-process signal profile, as well as to estimate the noisiness of the resulting gate function. Indeed, Figure 5 shows sample curves of the dependence of $F(t)$ on I_0 for a typical set of fitted parameters, $R = 208$ mM^{-1}, $r = 0.133$ mM^{-2}, for several fixed times. It is obvious that the logic zero for the output cannot be at the physical zero. However, in biomedical applications[53,58,59,92,93] this is not a disadvantage because both normal and pathophysiological concentrations of most biochemicals are typically nonzero.

If we select some reference value, $I_{1,2}(0) = I_{min}$, as logic-**0** of the inputs, and fix the gate-time, $t = t_g$ of the logic-gate processing, then for an accurate **XOR**, the value of $F_{min} = F(t = t_g; I_0 = 2I_{min})$ should also be obtainable at a larger, logic-**1** (for both inputs) $I_{1,2}(0) = I_{max}$, i.e., $F_{min} = F(t = t_g; I_0 = 2I_{max})$. This is obviously possible, because the curves in Figure 5 are nonmonotonic, as long as the selected I_{min} is not too small. However, then the logic-**1** value of the output, $F_{max} = F(t = t_g; I_0 = I_{min} + I_{max})$, will be at a certain large value but is not guaranteed to be close to the
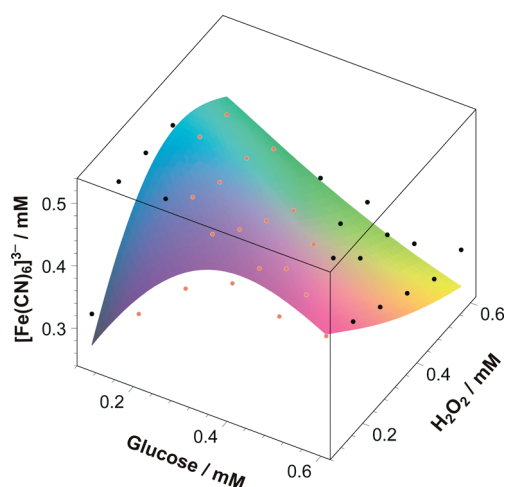
Figure 6. Model fit (surface) of the experimental data for the gate-function response shape (shown in terms of the physical, rather than scaled/shifted "logic" variables), at the selected gate time, 60 s. The black circles indicate the 17 data points which are above the level of the fitted surface. The orange circles mark the 19 data points which are below the level of the fitted surface. The data points have their horizontal-plain coordinates on a grid (not shown) defined by the 36 pairs of values at concentrations 0.1, 0.2, 0.3, 0.4, 0.5, and 0.6 mM along both the glucose and H_2O_2 axes.

maximum of the curve for the selected gate time. The result will be that the desired shape of Figure 3b, will not be well approximated as a "smoothed ridge." The response surface, which depicts the dependence of the scaled and shifted output variable

$$z = \frac{F - F_{min}}{F_{max} - F_{min}} \qquad (7)$$

on the similarly scaled and shifted inputs

$$x = \frac{I_1(0) - I_{min}}{I_{max} - I_{min}}, \quad y = \frac{I_2(0) - I_{min}}{I_{max} - I_{min}} \qquad (8)$$

will instead be asymmetrical and bulging above the level of the logic-1 for z, for certain inputs' (x and y) values between 0 and 1. The result will be large slopes and thus large analog-noise amplification for this type of gates. This is precisely the pattern of behavior found in our data, as described in the next section. Thus it is complicated/impractical to "optimize" by parameter selection/modification, the functioning of this type of **XOR** gates to achieve a smaller amplification factor (really close to the optimal ~140%) for analog noise in the inputs.

4. RESULTS AND DISCUSSION

Our data were taken as time-dependent sets measured for several values of both inputs. The data generally follow the pattern predicted by the semiquantitative model of section 3. An "optimization" by adjusting the parameters choices to get a response surface from which an **XOR** shape can be "cut out" which is not too asymmetrical and bulging as compared to Figure 3b, suggested the value $E(0) = 10^{-4}$ mM for the initial enzyme concentration used, as well as the choices of $I_{min} = 0.1$ mM, $I_{max} = 0.6$ mM, with the gate-time for the HRP processing step $t_g = 60$ s; see Figure 2. The measured data have

some noise and also do not exactly follow the analytical expression, 6, of our semiquantitative model.

The response surface at the selected gate-time was then mapped out based on the data for $I_{1,2} = 0.1, 0.2, 0.3, 0.4, 0.5,$ and 0.6 mM (total 36 data points). This gave the data depicted in Figure 6, which also shows the fitted surface according to the model eq 6. The model fit is semiquantitative, and here yield estimates $R = (208 \pm 14)$ mM^{-1}, $r = (0.133 \pm 0.013)$ mM^{-2} However, as emphasized in section 3, much larger variation of the rates is obtained if we consider separate time-dependent data sets.

Since the data are noisy and fluctuate about the fitted surface (see Figure 6), as mentioned in section 2 we used the experimental mean values of the logic-point **0** and **1** for the output, at the "logic" inputs, to define $F_{min} = 0.32$ mM, $F_{max} = 0.41$ mM, used in shifting and scaling the output, according to 7; see the bar chart in Figure 2. The values in this chart, and those in Figure 6 illustrate that there are several sources of noise in single-gate functioning. Specifically, the "logic" values of the output are not exactly at the desired numerical 0 and 1. Furthermore, the data are generally noisy, so that various experimental realizations do not even reproduce a smooth scaled surface $z(x,y)$, but rather a certain distribution of the z-values. However, as emphasized in earlier works,[27,60,81,82,85] for network functioning of the gate as part of complex information processing designs, noise amplification in the gate's signal processing is frequently more important than the noise-to-signal relative magnitude.

In order to estimate the analog noise amplification factor[27,60,81,82,85] assuming small spread of the noise in the inputs, we can use the absolute values of the gradients of the response surface function, $z(x,y)$, at the logic points. These gradient values were calculated for our fitted model surface, yielding 11.2, 0.6, 2.4, and 2.4, for the logic inputs **00**, **11**, **10**, **01**, respectively. We point out that had the data accurately approximated the "ridged" shape in Figure 3b, we would approach the optimal (for this type of gate) noise-amplification factor of $\sqrt{2} \approx 140\%$. However, we get (the largest, at **00**) factor of 11-fold amplification, $11.2 \approx 1100\%$. Thus, the realization is not optimal, and unfortunately, is not easy to improve in any significant way because of the numerous restrictions imposed on the parameter selection by the requirement of approximating the **XOR** truth table, 1, as described here and in section 3.

In conclusion, in this work we experimentally realized and theoretically modeled a new **XOR** function response, of the type shown in Figure 3b, for enzyme-based logic, which has the advantage of not requiring the postprocessing which is needed and was contemplated, but not yet experimentally realized for the earlier reported "signal change" **XOR**s approximating response of the type shown in Figure 3a. As with all the biochemical **XOR** functions based on single or few reaction steps, the realized gate function based on a substrate at larger concentrations inhibiting the enzyme's function, is noisy and, unlike **AND** or gates similar to it, cannot be as easily optimized at the biochemical reaction parameter level. Additional optimization by filtering and network design, as discussed elsewhere,[94,95] is needed for scalable functioning for complex information processing.

■ AUTHOR INFORMATION

Corresponding Author

*E-mail: ekatz@clarkson.edu. Tel.: +1 (315) 268-4421. Fax: +1 (315) 268-6610.

■ REFERENCES

(1) De Silva, A. P.; Uchiyama, S.; Vance, T. P.; Wannalerse, B. *Coord. Chem. Rev.* **2007**, *251*, 1623–1632.

(2) De Silva, A. P.; Uchiyama, S. *Nat. Nanotechnol.* **2007**, *2*, 399–410.

(3) Szacilowski, K. *Chem. Rev.* **2008**, *108*, 3481–3548.

(4) Credi, A. *Angew. Chem., Int. Ed.* **2007**, *46*, 5472–5475.

(5) Pischel, U. *Angew. Chem., Int. Ed.* **2007**, *46*, 4026–4040.

(6) Pischel, U. *Austral. J. Chem.* **2010**, *63*, 148–164.

(7) Andreasson, J.; Pischel, U. *Chem. Soc. Rev.* **2010**, *39*, 174–188.

(8) *Unconventional Computation. Lecture Notes in Computer Science.* Calude, C. S., Costa, J. F., Dershowitz, N., Freire, E., Rozenberg, G., Eds.; Springer: Berlin, 2009; Vol. 5715.

(9) *Unconventional Computing.* Adamatzky, A., De Lacy Costello, B., Bull, L., Stepney, S., Teuscher, C., Eds.; Luniver Press, U.K., 2007.

(10) De Silva, A. P.; Gunaratne, H. Q. N.; McCoy, C. P. *Nature* **1993**, *364*, 42–44.

(11) De Silva, A. P.; Gunaratne, H. Q. N.; McCoy, C. P. *J. Am. Chem. Soc.* **1997**, *119*, 7891–7892.

(12) De Silva, A. P.; Gunaratne, H. Q. N.; Maguire, G. E. M. *J. Chem. Soc., Chem. Commun.* **1994**, 1213–1214.

(13) Baytekin, H. T.; Akkaya, E. U. *Org. Lett.* **2000**, *2*, 1725–1727.

(14) Zong, G.; Xiana, L.; Lua, G. *Tetrahedron Lett.* **2007**, *48*, 3891–3894.

(15) De Silva, A. P.; Dixon, I. M.; Gunaratne, H. Q. N.; Gunnlaugsson, T.; Maxwell, P. R. S.; Rice, T. E. *J. Am. Chem. Soc.* **1999**, *121*, 1393–1394.

(16) Straight, S. D.; Liddell, P. A.; Terazono, Y.; Moore, T. A.; Moore, A. L.; Gust, D. *Adv. Funct. Mater.* **2007**, *17*, 777–785.

(17) Turfan, B.; Akkaya, E. U. *Org. Lett.* **2002**, *4*, 2857–2859.

(18) Wang, Z.; Zheng, G.; Lu, P. *Org. Lett.* **2005**, *7*, 3669–3672.

(19) Gunnlaugsson, T.; Mac Dónaill, D. A.; Parker, D. *J. Am. Chem. Soc.* **2001**, *123*, 12866–12876.

(20) Gunnlaugsson, T.; MacDónaill, D. A.; Parker, D. *Chem. Commun.* **2000**, 93–94.

(21) De Sousa, M.; De Castro, B.; Abad, S.; Miranda, M. A.; Pischel, U. *Chem. Commun.* **2006**, 2051–2053.

(22) Li, L.; Yu, M. X.; Li, F. Y.; Yi, T.; Huang, C. H. *Colloids Surf. A* **2007**, *304*, 49–53.

(23) Credi, A.; Balzani, V.; Langford, S. J.; Stoddart, J. F. *J. Am. Chem. Soc.* **1997**, *119*, 2679–2681.

(24) Li, Y.; Zheng, H.; Li, Y.; Wang, S.; Wu, Z.; Liu, P.; Gao, Z.; Liu, H.; Zhu, D. *J. Org. Chem.* **2007**, *72*, 2878–2885.

(25) De Silva, A. P.; McClenaghan, N. D. *Chem.—Eur. J.* **2002**, *8*, 4935–4945.

(26) De Silva, A. P.; McClenaghan, N. D. *J. Am. Chem. Soc.* **2000**, *122*, 3965–3966.

(27) Katz, E.; Privman, V. *Chem. Soc. Rev.* **2010**, *39*, 1835–1857.

(28) Saghatelian, A.; Volcker, N. H.; Guckian, K. M.; Lin, V. S. Y.; Ghadiri, M. R. *J. Am. Chem. Soc.* **2003**, *125*, 346–347.

(29) Ashkenasy, G.; Ghadiri, M. R. *J. Am. Chem. Soc.* **2004**, *126*, 11140–11141.

(30) Sivan, S.; Lotan, N. *Biotechnol. Prog.* **1999**, *15*, 964–970.

(31) Sivan, S.; Tuchman, S.; Lotan, N. *Biosystems* **2003**, *70*, 21–33.

(32) Deonarine, A. S.; Clark, S. M.; Konermann, L. *Future Gener. Comput. Syst.* **2003**, *19*, 87–97.

(33) Ashkenazi, G.; Ripoll, D. R.; Lotan, N.; Scheraga, H. A. *Biosens. Bioelectron.* **1997**, *12*, 85–95.

(34) Unger, R.; Moult, J. *Proteins* **2006**, *63*, 53–64.

(35) Zhou, J.; Arugula, M. A.; Halámek, J.; Pita, M.; Katz, E. *J. Phys. Chem. B* **2009**, *113*, 16065–16070.

(36) Zhou, J.; Tam, T. K.; Pita, M.; Ornatska, M.; Minko, S.; Katz, E. *ACS Appl. Mater. Interfaces* **2009**, *1*, 144–149.

(37) Strack, G.; Ornatska, M.; Pita, M.; Katz, E. *J. Am. Chem. Soc.* **2008**, *130*, 4234–4235.

(38) Pita, M.; Katz, E. *J. Am. Chem. Soc.* **2008**, *130*, 36–37.

(39) Strack, G.; Chinnapareddy, S.; Volkov, D.; Halámek, J.; Pita, M.; Sokolov, I.; Katz, E. *J. Phys. Chem. B* **2009**, *113*, 12154–12159.

(40) Tam, T. K.; Strack, G.; Pita, M.; Katz, E. *J. Am. Chem. Soc.* **2009**, *131*, 11670–11671.

(41) Li, T.; Wang, E. K.; Dong, S. J. *J. Am. Chem. Soc.* **2009**, *131*, 15082–15083.

(42) Willner, I.; Shlyahovsky, B.; Zayats, M.; Willner, B. *Chem. Soc. Rev.* **2008**, *37*, 1153–1165.

(43) Stojanovic, M. N.; Stefanovic, D.; LaBean, T.; Yan, H. in *Bioelectronics: From Theory to Applications*; Willner, I., Katz, E., Eds.; Wiley-VCH: Weinheim, Germany, 2005; pp 427–455.

(44) Ezziane, Z. *Nanotechnology* **2006**, *17*, R27–R39.

(45) Win, M. N.; Smolke, C. D. *Science* **2008**, *322*, 456–460.

(46) Rinaudo, K.; Bleris, L.; Maddamsetti, R.; Subramanian, S.; Weiss, R.; Benenson, Y. *Nat. Biotechnol.* **2007**, *25*, 795–801.

(47) Ogawa, A.; Maeda, M. *Chem. Commun.* **2009**, 4666–4668.

(48) Stojanovic, M. N.; Mitchell, T. E.; Stefanovic, D. *J. Am. Chem. Soc.* **2002**, *124*, 3555–3561.

(49) Benenson, Y. *Curr. Opin. Biotechnol.* **2009**, *20*, 471–478.

(50) Simpson, M. L.; Sayler, G. S.; Fleming, J. T.; Applegate, B. *Trends Biotechnol.* **2001**, *19*, 317–323.

(51) Margulies, D.; Hamilton, A. D. *J. Am. Chem. Soc.* **2009**, *131*, 9142–9143.

(52) May, E. E.; Dolan, P. L.; Crozier, P. S.; Brozik, S.; Manginell, M. *IEEE Sens. J.* **2008**, *8*, 1011–1019.

(53) Wang, J.; Katz, E. *Anal. Bioanal. Chem.* **2010**, *398*, 1591–1603.

(54) Strack, G.; Bocharova, V.; Arugula, M. A.; Pita, M.; Halámek, J.; Katz, E. *J. Phys. Chem. Lett.* **2010**, *1*, 839–843.

(55) Tokarev, I.; Gopishetty, V.; Zhou, J.; Pita, M.; Motornov, M.; Katz, E.; Minko, S. *ACS Appl. Mater. Interfaces* **2009**, *1*, 532–536.

(56) Simmel, F. C. *Nanomedicine* **2007**, *2*, 817–830.

(57) von Maltzahn, G.; Harris, T. J.; Park, J.-H.; Min, D.-H.; Schmidt, A. J.; Sailor, M. J.; Bhatia, S. N. *J. Am. Chem. Soc.* **2007**, *129*, 6064–6065.

(58) Manesh, K. M.; Halámek, J.; Pita, M.; Zhou, J.; Tam, T. K.; Santhosh, P.; Chuang, M.-C.; Windmiller, J. R.; Abidin, D.; Katz, E.; Wang, J. *Biosens. Bioelectron.* **2009**, *24*, 3569–3574.

(59) Pita, M.; Zhou, J.; Manesh, K. M.; Halámek, J.; Katz, E.; Wang, J. *Sens. Actuat. B* **2009**, *139*, 631–636.

(60) Privman, V.; Zhou, J.; Halámek, J.; Katz, E. *J. Phys. Chem. B* **2010**, *114*, 13601–13608.

(61) Strack, G.; Pita, M.; Ornatska, M.; Katz, E. *ChemBioChem* **2008**, *9*, 1260–1266.

(62) Baron, R.; Lioubashevski, O.; Katz, E.; Niazov, T.; Willner, I. *J. Phys. Chem. A* **2006**, *110*, 8548–8553.

(63) Niazov, T.; Baron, R.; Katz, E.; Lioubashevski, O.; Willner, I. *Proc. Natl. Acad. Sci. U.S.A.* **2006**, *103*, 17160–17163.

(64) Baron, R.; Lioubashevski, O.; Katz, E.; Niazov, T.; Willner, I. *Angew. Chem., Int. Ed.* **2006**, *45*, 1572–1576.

(65) Qu, D.-H.; Wang, Q.-C.; Tian, H. *Angew. Chem., Int. Ed.* **2005**, *44*, 5296–5299.

(66) Andréasson, J.; Straight, S. D.; Kodis, G.; Park, C.-D.; Hambourger, M.; Gervaldo, M.; Albinsson, B.; Moore, T. A.; Moore, A. L.; Gust, D. *J. Am. Chem. Soc.* **2006**, *128*, 16259–16265.

(67) Andréasson, J.; Kodis, G.; Terazono, Y.; Liddell, P. A.; Bandyopadhyay, S.; Mitchell, R. H.; Moore, T. A.; Moore, A. L.; Gust, D. *J. Am. Chem. Soc.* **2004**, *126*, 15926–15927.

(68) Lopez, M. V.; Vazquez, M. E.; Gomez-Reino, C.; Pedrido, R.; Bermejo, M. R. *New J. Chem.* **2008**, *32*, 1473–1477.

(69) Margulies, D.; Melman, G.; Shanzer, A. *J. Am. Chem. Soc.* **2006**, *128*, 4865–4871.

(70) Kuznetz, O.; Salman, H.; Shakkour, N.; Eichen, Y.; Speiser, S. *Chem. Phys. Lett.* **2008**, *451*, 63–67.

(71) Ho, M. S. H.; Lin, J.; Chiu, C. C. *Int. J. Innovative Comput. Informat. Control* **2009**, *5*, 4573–4582.

(72) Fredkin, E.; Toffoli, T. *Int. J. Theor. Phys.* **1982**, *21*, 219–253.

(73) Donald, J.; Jha, N. K. *ACM Journal on Emerging Technologies in Computing Systems* **2008**, *4*, art. #2.

9844

dx.doi.org/10.1021/jp2041372 |*J. Phys. Chem. B* 2011, 115, 9838–9845

(74) Shende, V. V.; Markov, I. L. *Quantum Informat. Comput.* **2009**, *9*, 461–486.

(75) Bennett, C. H. *IBM J. Res. Dev.* **1973**, *17*, 525–532.

(76) Ekert, A.; Jozsa, R. *Rev. Mod. Phys.* **1996**, *68*, 733–753.

(77) Steane, A. M. *Rept. Prog. Phys.* **1998**, *61*, 117–173.

(78) Morpurgo, L.; Hartmann, H. J.; Desideri, A.; Weser, U.; Rotilio, G. *Biochem. J.* **1983**, *211*, 515–517.

(79) Maethly, A. C. *Methods Enzymol.* **1953**, *2*, 801–813.

(80) Kamal, J. K. A.; Behere, D. V. *J. Inorg. Biochem.* **2003**, *94*, 236–242.

(81) Privman, V.; Strack, G.; Solenov, D.; Pita, M.; Katz, E. *J. Phys. Chem. B* **2008**, *112*, 11777–11784.

(82) Privman, V.; Pedrosa, V.; Melnikov, D.; Pita, M.; Simonian, A.; Katz, E. *Biosens. Bioelectron.* **2009**, *25*, 695–701.

(83) Renjun, P.; Matamoros, E.; Liu, M.; Stefanovic, D.; Stojanovic, M. N. *Nat. Nanotechnol.* **2010**, *5*, 773–777.

(84) Privman, V. *Nat. Nanotechnol.* **2010**, *5*, 767–768.

(85) Privman, V. *Israel J. Chem.* **2010**, *51*, 118–131.

(86) Hasinoff, B. B.; Dunfordt, H. B. *Biochemistry* **1970**, *25*, 4930–4939.

(87) Arnao, M. B.; Acosta, M.; del Rió, J. A.; Varón, R.; García-Cánovas, F. *Biochim. Biophys. Acta* **1990**, *1041*, 43–47.

(88) Nicell, J. A.; Wright, H. *Enzyme Microb. Technol.* **1997**, *21*, 302–310.

(89) Berezin, I. V; Levashov, A.; Martinek, K. *Eur. J. Biochem.* **1970**, *16*, 472–474.

(90) Berezin, I. V; Varfolomeyev, S. D.; Klibanov, A. M.; Martinek, K. *FEBS Lett.* **1974**, *39*, 329–331.

(91) Varfolomeyev, S. D.; Kazanskaya, N. F.; Eremeev, N. L. *BioSystems* **1996**, *39*, 35–42.

(92) Halámek, J.; Windmiller, J. R.; Zhou, J.; Chuang, M.-C.; Santhosh, P.; Strack, G.; Arugula, M. A.; Chinnapareddy, S.; Bocharova, V.; Wang, J.; Katz, E. *Analyst* **2010**, *135*, 2249–2259.

(93) Melnikov, D.; Strack, G.; Zhou, J.; Windmiller, J. R.; Halámek, J.; Bocharova, V.; Chuang, M.-C.; Santhosh, P.; Privman, V.; Wang, J.; Katz, E. *J. Phys. Chem. B* **2010**, *114*, 12166–12174.

(94) Privman, V.; Halámek, J.; Arugula, M. A.; Melnikov, D.; Bocharova, V.; Katz, E. *J. Phys. Chem. B* **2010**, *114*, 14103–14109.

(95) Pita, M.; Privman, V.; Arugula, M. A.; Melnikov, D.; Bocharova, V.; Katz, E. *Phys. Chem. Chem. Phys.* **2011**, *13*, 4507–4513.